LBL-29389
TA-275

Published in Solar Energy Materials 20 (1990) pp. 277-288, North Holland, Elsevier Science Publishers B.V.

The Effects of Infrared Absorbing Gasses on Window Heat Transfer: A Comparison of Theory and Experiment

M.S. Reilly, D. Arasteh, and M. Rubin
Windows and Daylighting Group
Applied Science Division
Lawrence Berkeley Laboratory
1 Cyclotron Road, Building 90, Room 3111
Berkeley, California 94720

November 1989

This work was supported by the Assistant Secretary for Conservation and Renewable Energy, Office of Building Technologies, Building Systems and Materials Division, U.S. Department of Energy under Contract No. DE-AC03-76SF00098.

THE EFFECTS OF INFRARED ABSORBING GASSES ON WINDOW HEAT TRANSFER: A COMPARISON OF THEORY AND EXPERIMENT

Susan REILLY, Dariush ARASTEH and Mike RUBIN

Lawrence Berkeley Laboratory (MS 90-3111), Windows and Daylighting Group, Berkeley, CA 94720, USA

This paper extends an existing heat transfer model of multipane windows filled with gasses to include the effects of infrared absorption within the gasses. A one-dimensional, finite-element, control-volume approach for calculating the heat transfer across a horizontal window filled with an infrared absorbing gas is presented. This model includes the coupled effects of conduction and radiation but not convection. Experimental data on the heat transfer rates through windows filled with infrared absorbing gasses and heated from above (to minimize convection) agree with results from this model. Infrared absorbing gasses are shown to have a small effect on reducing heat transfer through common window systems and are not as effective as low-emittance coatings for reducing radiative heat transfer.

1. Introduction

Calculating the one-dimensional heat transfer through a window assuming steady-state conditions and neglecting the edge effects is well understood for windows filled with non-absorbing gasses [1,2]. The complexity introduced into the calculations by infrared absorbing gasses is due to the spectral dependence of the infrared absorptivity. The problem becomes one of coupled conductive, convective, and radiative heat transfer since all heat transfer modes are temperature dependent. The contribution of incident solar radiation to the energy balance further complicates the analysis.

Until now, the work done in this field has focused either on the total heat transfer through a window [3] or solely on the infrared absorption of gasses [4]. Our work addresses the relative contributions of conduction and radiation in a window filled with an absorbing gas, and looks at the influence of natural convection as exhibited by the experimental work of Glaser [3].

We first consider a horizontal, double-pane window heated from above. This negates any natural convection effects in the space separating the two panes, so only conductive and radiative heat transfer occurs in the space. Exterior air temperatures are specified along with film coefficients for the two outwardly-facing surfaces in accordance with Glaser's experimental work [3].

Various methods exist for calculating the radiation heat transfer across two parallel plates separated by an absorbing gas. Different working assumptions which

distinguish some of these methods, such as the optically-thin case, the optically-thick case, and the gray gas case are inappropriate for the absorbing gasses considered here [5]. In the gray gas case, the optical properties of the gas do not vary with wavelength. A method proven preferable to a gray gas approximation is a band formulation, which describes the properties of each absorption band of a gas. The band formulation adopted here is Edwards exponential wide-band model [6]. This model relies on three parameters to obtain the band absorption, and these parameters are known for SF_6 [7], CO_2 [6], NH_3 [8], and N_2O [9], and some other gasses [7].

We incorporated Edwards wide-band formulation into a one-dimensional, finite-element, control-volume approach to find the temperature distribution across a window. It is possible to handle the gasses mentioned above with this model, and also mixtures of these gasses with each other and with non-absorbing gasses [10]. Results from this model are compared to both Glaser's experimental results and WINDOW 3.1 results for air, SF_6, and CO_2. WINDOW 3.1 is a computer program for calculating the heat transfer through windows. It does not account for absorption effects [11]. An ammonia(NH_3)-filled window is also evaluated with the model and WINDOW 3.1, solely as an example of a more strongly absorbing gas. Due to its toxicity, NH_3 is not a practical gas-fill.

2. Heat transfer model

To evaluate the heat transfer through a double-glazed window filled with an infrared absorbing gas, we first approximate the window as two horizontal, infinite-parallel-glass panes exposed to fixed air temperatures on the outwardly-facing surfaces (fig. 1). T_{out} and T_{in} refer to the outside and inside air temperatures respectively with $T_{out} < T_{in}$. The space between the glass panes is gas-filled, the width of which ranges from 6 to 20 mm. We must solve for the steady-state temperature distribution across this system.

The infrared optical properties of each glass surface are necessary for calculating the thermal radiation leaving these surfaces. Hemispherical-average properties are used since the glass properties are nearly constant over the infrared spectrum. We examine two cases: (1) the uncoated-glass case; and (2) the coated-glass case. The coated-glass case refers to a thin, metallic film (low-emittance coating) which is applied to one of the glass surfaces. The film is transparent throughout the solar

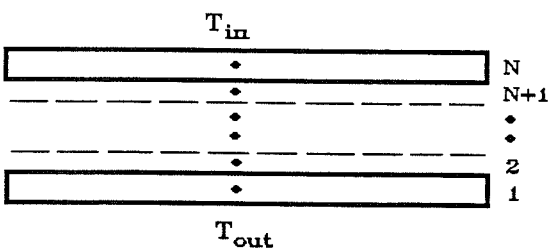

Fig. 1. Schematic of a horizontal, double-pane window where $T_{out} < T_{in}$. The window is divided into N temperature nodes.

spectrum, and is highly reflective in the infrared spectrum (has a low emittance). The infrared transmittance of coated and uncoated glass is zero. Uncoated clear-silica glass has a hemispherical surface emittance of 0.84. In the coated-glass case, the surface that faces the gas layer of the glass pane exposed to T_{in} is assumed to have an emittance of 0.065, which is representative of a gold coating.

The gas space is divided into $N-2$ isothermal layers and a temperature node is associated with each layer. A temperature node is assigned to each glass pane also, thus giving N nodes (fig. 1). The one-dimensional, finite-element model iteratively solves for the temperature distribution by performing an energy balance at each node. The convergence criteria requires that the energy flux leaving the exterior surfaces agree to within 0.5 W/m^2 (approximately 2% of the surface heat transfer) with each other, and that the residual from each energy balance be less than 0.2 W/m^2.

Each gas layer conducts energy and transmits, absorbs and emits thermal radiation; and the glass reflects, absorbs and emits thermal radiation. The model ignores conduction through the glass because most glazing materials have a relatively insignificant resistance to heat flow as compared to the surrounding gas layers [1].

2.1. Radiation exchange within the absorption bands

Consider two surfaces bounding each node, so for N nodes there are $2N$ surfaces. First, calculate the net infrared energy flux leaving the $2n$ and $2n-1$ surfaces of temperature node n for each absorption band, Q_i^a from:

$$Q_{2n}^a = S_{2n} + R_{2n}Q_{2n+1}^a + T_nQ_{2n-2}^a, \tag{1}$$

$$Q_{2n-1}^a = S_{2n-1} + R_{2n-1}Q_{2n-2}^a + T_nQ_{2n+1}^a, \tag{2}$$

where S_i represents the energy emitted from the ith surface. The infrared reflectance, R, of the gas layer surfaces is zero and the infrared transmittance, T, of the glass is zero. The transmittance of each gas band is approximated by [5]

$$T = 1 - A/\Delta\omega, \tag{3}$$

where A is the integrated absorptance from the wide-band formulation for a particular band and $\Delta\omega$ signifies the wavelength range for that band.

Table 1 lists the band limits used for CO_2 and SF_6 in the heat transfer calculations. The band limits for NH_3 can be found in ref. [5]. The band limits of the absorption bands of any gas are generally not well-defined. A formula presented by Edwards for parallel plate geometry for computing the wavelength range of a band is used [12]. The limits obtained from this formula agree well with those listed for CO_2, but care must be taken when the limits of bands overlap.

The infrared energy flux leaving the outside and inside surroundings within each absorption band, Q_0^a and Q_{2N+1}^a, are renamed Q_{out}^a and Q_{in}^a. The emittances of the outside and inside, ϵ_{out} and ϵ_{in}, are 1.0.

Eqs. (1) and (2) form a set of N pair of equations for each important absorptance band in a gas. Rearranging this inhomogeneous linear set of equations into matrix

Table 1
Band limits for CO_2 and SF_6

Gas	Ref.	Band limits (cm^{-1})		
		Band center	Lower	Upper
CO_2	[5]	667	$667-A/1.78$	$667+A/1.78$
		960	849	1013
		1060	1013	1141
		2350	$2350-A/1.78$	2430
		3715	$3715-A/1.78$	3750
SF_6	[12,13]	615	$615-\Delta\omega/2$	$615+\Delta\omega/2$
		870	$870-\Delta\omega/2$	903
		948	903	968
		991	968	1013
		1588	$1588-\Delta\omega/2$	$1588+\Delta\omega/2$
		1720	1690	1725

A is the integrated band absorptance, and $\Delta\omega$ is the wavelength range over which the gas is absorbing. Refer to ref. [12] for approximating $\Delta\omega$.

form gives

$$\sum M_{ij} Q_j^a = S_i. \tag{4}$$

The $2N$ by $2N$ matrix $[M]$ contains:

$$M_{ii} = 1, \tag{5}$$

$$M_{2n-1,2n-2} = -R_{2n-1}, \tag{6}$$

$$M_{2n-1,2n+2} = -T_n, \tag{7}$$

$$M_{2n,2n-2} = -T_n, \tag{8}$$

$$M_{2n,2n+1} = -R_{2n}. \tag{9}$$

All other elements are zero. By assuming the temperature of each layer, the energy emitted by each surface or the source term, S_i, specific to an absorptance band is found from Planck's law:

$$S_i = \frac{2\pi C_1 \nu^3}{e^{C_2\nu/T} - 1} d\nu, \tag{10}$$

which is the hemispherical emissive power, where C_1 equals 0.59544×10^8 W $\mu m^4/m^2$ and C_2 equals 14388 μm K. The wavenumber, ν, represents the band center in cm^{-1}, T is the gas temperature in Kelvin, and $d\nu$ refers to the band region over which the gas is absorbing (cm^{-1}). The source terms leaving the glass surfaces and from the inside and outside surroundings are calculated within the band limits.

The net radiative flux leaving the surface within each absorption band is computed from

$$Q_i^a = \sum (M^{-1})_{ij} S_j. \tag{11}$$

Eqs. (1)–(11) are performed for each absorption band. The Q_i^a computed for the individual bands are summed up within each gas layer to give a total net radiation flux leaving each gas-layer surface for the absorbing regions, Q_i^A.

2.2. Radiation exchange outside of the absorption bands

Only the glass surfaces 1, 2, $2N-1$, and $2N$ have radiative flux terms, Q_i^R within the non-absorbing regions. These terms are

$$Q_1^R = S_1^R + R_1 S_{out}^R, \tag{12}$$

$$Q_2^R = S_2^R + R_2 Q_{2N-1}^R, \tag{13}$$

$$Q_{2N-1}^R = S_{2N-1}^R + R_{2N-1} Q_2^R, \tag{14}$$

$$Q_{2N}^R = S_{2N}^R + R_{2N} S_{in}^R, \tag{15}$$

where S_{in}^R and S_{out}^R refer to the blackbody radiation emitted at temperatures T_{in} and T_{out} over the non-absorbing regions. Simultaneously solving Q_2^R and Q_{2N-1}^R gives

$$Q_2^R = \frac{S_2^R + R_2 S_{2N-1}^R}{1 - R_2 R_{2N-1}}, \tag{16}$$

$$Q_{2N-1}^R = \frac{S_{2N-1}^R + R_2 S_2^R}{1 - R_2 R_{2N-1}}. \tag{17}$$

The source terms, S_i^R, are estimated using Wiebelt's formula for calculating the fraction of blackbody emissive power between 0 and λ, $F_{0-\lambda T}$ [14]:

$$F_{0-\lambda T} = \frac{15}{\pi^4} \frac{e^{-mv}}{m^4} \left[(mv+3)mv + 6 \right], \quad v \geq 2, \tag{18}$$

$$F_{0-\lambda T} = 1 - \frac{15}{\pi^4} v^3 \left(\frac{1}{3} - \frac{v}{8} + \frac{v^2}{60} - \frac{v^4}{5040} + \frac{v^6}{272\,160} - \frac{v^8}{13\,305\,600} \right), \quad v < 2, \tag{19}$$

where

$$v = \frac{C_2}{\lambda T}. \tag{20}$$

C_2 is the same constant as in Planck's law, λ is the wavelength of the upper or lower band limit, and T is the temperature. The total fraction of blackbody emissive power emitted by one of these surfaces equals the sum of the differences between successive upper and lower band limits. Multiply this fraction by the total blackbody emissive power and the surface emittance to obtain the emitted radiative flux outside the absorption bands, S_i^R. From the Stefan–Boltzmann law, the hemispherical total emissive power, e_b, is

$$e_b = \sigma T^4, \tag{21}$$

where σ is the Stefan–Boltzmann constant and T is the temperature. Note that S_i^R is zero for the gas layers.

2.3. Conduction

Linearizing the equation for the conduction component between successive nodes gives

$$Q_{2n}^{C} = -k\frac{\Delta T_{(n+1)-n}}{\Delta x_{(n+1)-n}}, \tag{22}$$

where the thermal conductivity of the gas, k, is considered constant, $\Delta T_{(n+1)-n}$ equals the temperature difference and $\Delta x_{(n+1)-n}$ refers to the distance between successive nodes.

2.4. Heat transfer from the surroundings

The heat transfer from the exterior-facing surfaces of the glass due to convection/conduction is approximated by film coefficients which Glaser assumed. The coefficient for the surface seeing T_0 is 25.0 $W/m^2 \cdot K$, and the coefficient for the surface exposed to T_i is 8.33 $W/m^2 \cdot K$ [3]. These film coefficients include the radiative component and must be modified to yield h_0 and h_i. So, the conductive/convective energy flux leaving surface 1, Q_1^C, and surface $2N$, Q_{2N}^C, are

$$Q_1^C = h_0(T_1 - T_0), \tag{23}$$

$$Q_{2N}^C = h_i(T_N - T_i). \tag{24}$$

2.5. Energy balance

The finite-element model calculates each of the energy terms and performs an energy balance at each node. For the gas nodes, the residual of the energy balance, Δ_n, equals

$$\Delta_n = Q_{2n}^A + Q_{2n-1}^A - Q_{2n+1}^A - Q_{2n-2}^A + Q_{2n}^C - Q_{2n-1}^C, \tag{25}$$

and for the glass nodes the residuals equal

$$\Delta_1 = Q_1^R + Q_2^R - Q_{out}^R - Q_{2N-1}^R + Q_1^A + Q_2^A - Q_{out}^A - Q_3^A + Q_1^C - Q_2^C, \tag{26}$$

$$\Delta_N = Q_{2N-1}^R + Q_{2N}^R - Q_{in}^R - Q_2^R + Q_{2N-1}^A + Q_{2N}^A - Q_{in}^A - Q_{2N-2}^A + Q_{2N-1}^C - Q_{2N}^C. \tag{27}$$

3. Results

Windows are rated by U-value, U ($W/m^2 \cdot K$), and the total flux through a window equals

$$Q = U(T_{in} - T_{out}). \tag{28}$$

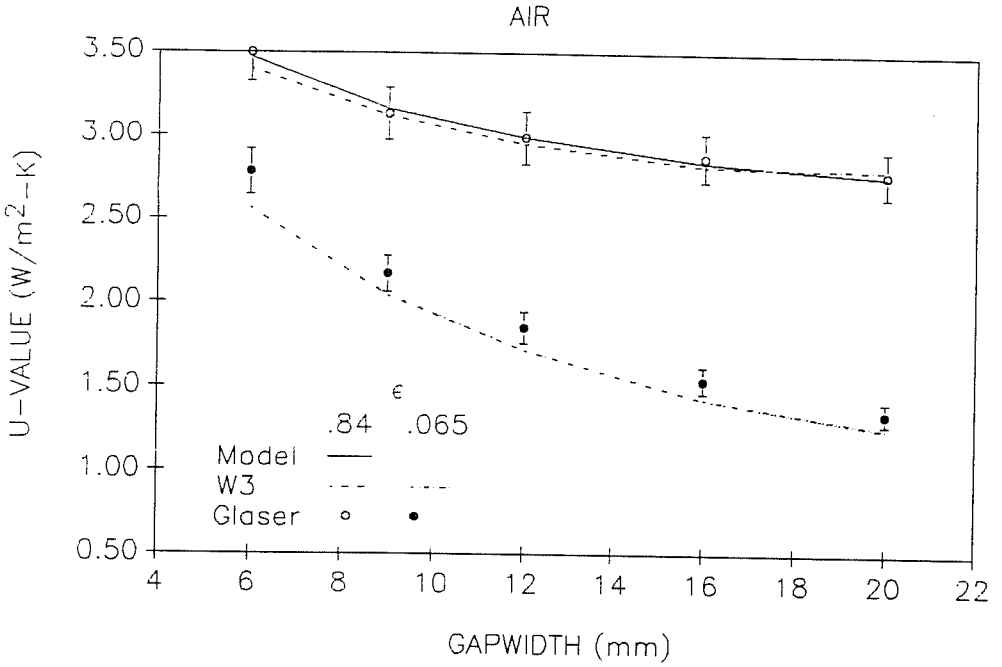

Fig. 2. *U*-values calculated by the finite-element model and WINDOW 3.1, and measured by Glaser for horizontal windows filled with air.

The *U*-values for air, CO_2, and SF_6, as calculated by WINDOW 3.1 (no infrared absorbing effects) and the finite-element model (includes infrared absorbing effects), are compared to Glaser's findings for a horizontal window. Glaser conducted hot plate experiments on a double-pane window. He set up a 10 ± 0.5 K temperature difference across the window with a mean temperature of 283 K and ran tests with assorted gas-fills for both vertical and horizontal positions. The windows are heated from above in the horizontal position to eliminate natural convection in the gas layer.

Figs. 2–4 compare the results from the three methods. WINDOW 3.1 has been verified for air and other non-absorbing gasses [15], and the agreement between the results from the finite-element model and WINDOW 3.1 for air ensures that the finite-element model calculations are accurate for non-absorbing gasses (fig. 2). For the uncoated-glass case, WINDOW 3.1 and the finite-element model results agree with Glaser to within experimental error ($\pm 5\%$). For the coated-glass case, both WINDOW 3.1 and the finite-element model consistently predict lower values than Glaser found for air, SF_6, and CO_2. In a comparison of WINDOW 3.1 predictions and experimental data by Arasteh, Hartmann and Rubin [15], they speculated that the coating emittance could be higher than that reported by Glaser; an emittance value of 0.065 is very low and coating emittances often vary by ± 0.02–0.03. With a surface emittance of 0.1, WINDOW 3.1 calculates values that give very good agreement with Glaser.

The difference in the results of the finite-element model and WINDOW 3.1 can be attributed to infrared absorption and emission by the gas since WINDOW 3.1

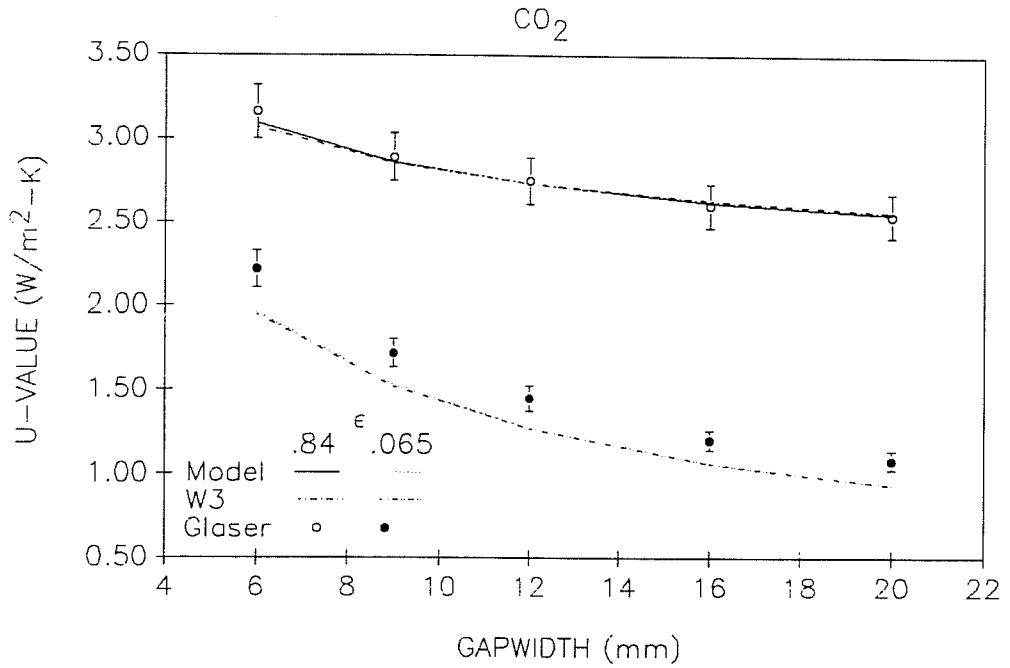

Fig. 3. *U*-values calculated by the finite-element model and WINDOW 3.1, and measured by Glaser for horizontal windows filled with CO_2.

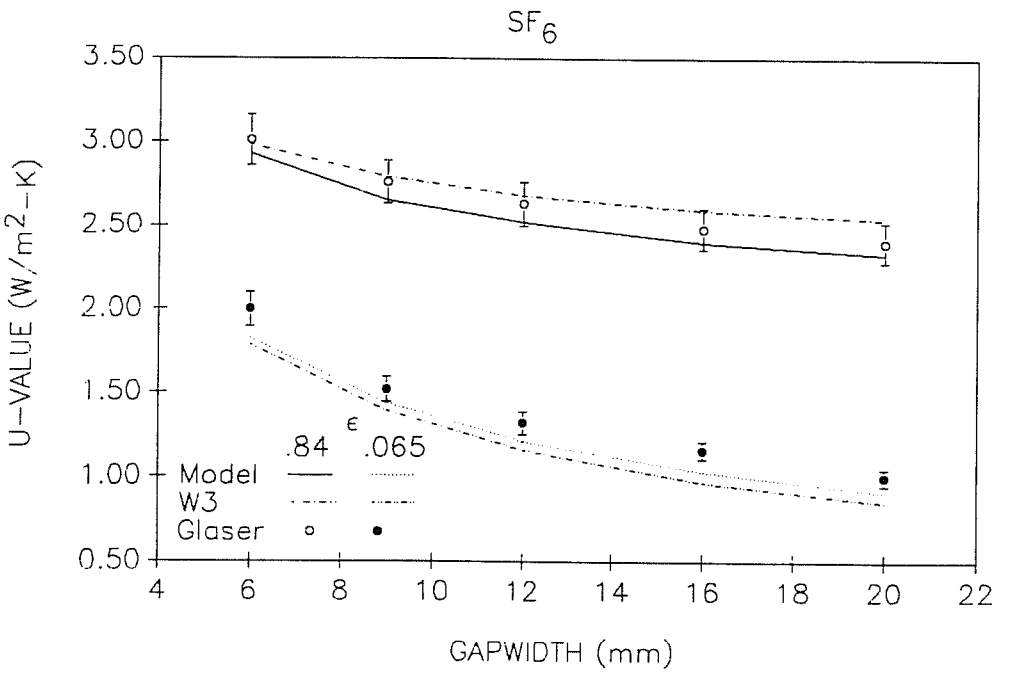

Fig. 4. *U*-values calculated by the finite-element model and WINDOW 3.1, and measured by Glaser for horizontal windows filled with SF_6.

assumes all gasses are non-absorbing. Fig. 3 shows that the effect of the infrared radiation properties of CO_2 is unnoticeable, while fig. 4 shows a noticeable effect with SF_6. For the uncoated-glass case in which radiative transfer dominates, there is a 2% decrease in the *U*-value at 6 mm and an 8% decrease at 20 mm over what WINDOW 3.1 predicts for SF_6. For the coated-glass case conductive transfer dominates and the infrared radiative transfer between the surfaces is small. The gas, however, emits infrared radiation thus degrading the performance of the SF_6-filled window. The model predicts values that are 2% to 7% higher than what WINDOW 3.1 predicts.

Glaser performed experiments on vertical windows as well, so it is possible to observe the influence of natural convection within the gap. In fig. 5, Glaser's results for air and SF_6 for a vertical window are presented along with WINDOW 3.1 results. The discrepancy between the two sets of results for SF_6 is greater than for the horizontal windows, and is attributed primarily to the natural convection correlations within WINDOW 3.1 for the gas layer. These correlations are accurate for non-absorbing gasses, but do not reflect the effect of infrared absorption on the temperature gradient. Notice that for the coated-glass case, WINDOW 3.1 gives higher *U*-values than what Glaser measured, although for the horizontal windows WINDOW 3.1 calculated lower values. Kim and Viskanta show that the temperature gradient in the fluid and thus the local Nusselt number decreases as the wall emissivity increases [16]. This effect on natural convection, plus the fact that the gas is emitting radiation which would also decrease the fluid temperature gradient need to be accounted for. One could also expect the gas absorption in the uncoated-glass

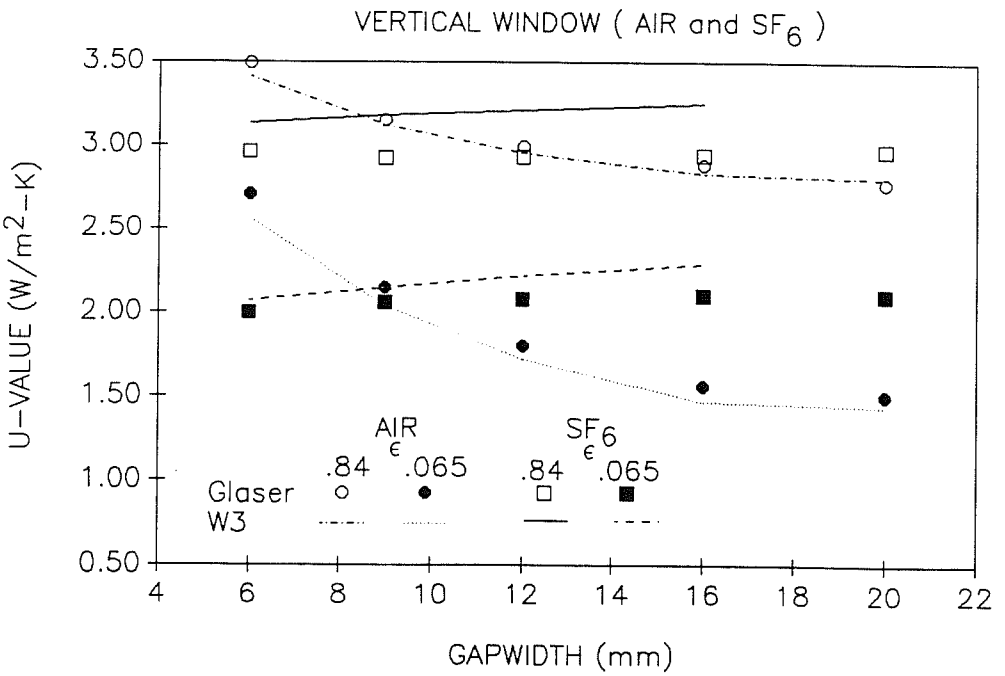

Fig. 5. *U*-values measured by Glaser and calculated by WINDOW 3.1 for vertical windows filled with air or SF_6.

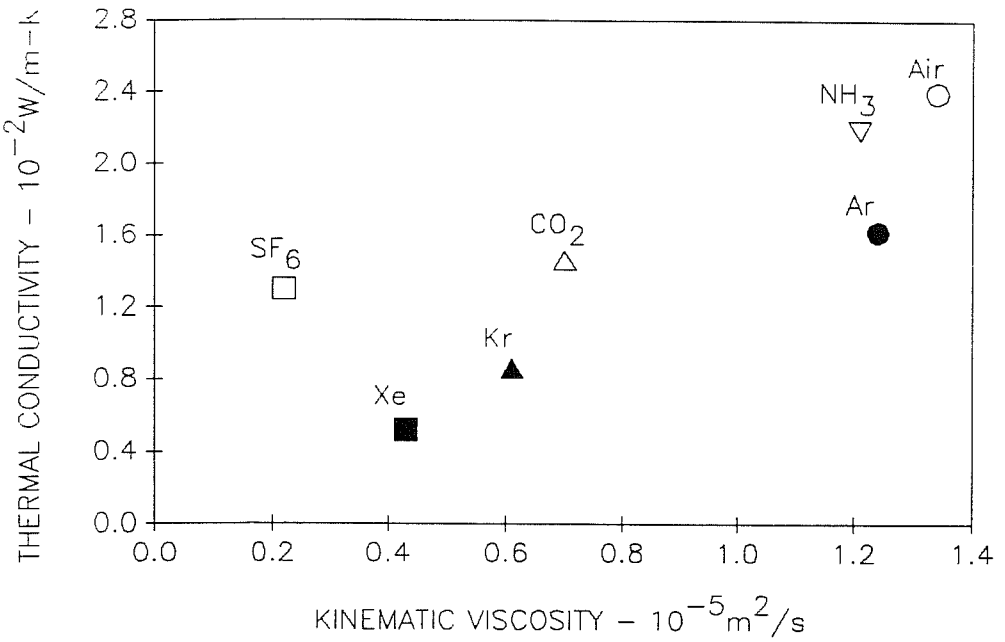

Fig. 6. Conductivity and kinematic viscosity of pure gasses [17].

case to decrease the fluid temperature gradient. However, even though the gas absorption/emission dampens the natural convection, the absorbing gasses being used as gas-fills have lower kinematic viscosities than air and some of the other low-conductivity gasses (argon, krypton) being used in windows (fig. 6). And, from Glaser's results for vertical windows it can be seen that the convective transfer becomes significant at around 9 mm for SF_6, while there is practically no convective transfer through an air-filled window at gapwidths up to 20 mm under these conditions. In fact, air outperforms SF_6 at gapwidths greater than 9 mm in a vertical window and the benefits from infrared absorption by SF_6 have been negated by the magnitude of the convection.

When low-emittance coatings are used, conductive and convective heat transfer losses determine window thermal performance. So gas-fills for such windows should have a low thermal conductivity and a high kinematic viscosity. Not only do the absorbing gasses generally have low kinematic viscosities, but the infrared emission from the gas adversely affects the window performance. Most importantly though, is that low-emittance coatings appear to be much more effective at reducing radiative transfer than absorbing gasses. Fig. 7 compares WINDOW 3.1 and the finite-element model results for NH_3 with those for an air-filled, double-pane, low-e window. The low-emittance film has an emittance of 0.4 which is representative of a mediocre, pyrolytic coating. NH_3 was chosen since it is a highly absorbing gas. (Note that the conductivity and kinematic viscosity of NH_3 are close to those of air.) For the uncoated-glass case, the finite-element model predicts *U*-values that are 8% at 6 mm and 26% at 20 mm lower than what WINDOW 3.1 calculates for NH_3, which is an indication of the effect of infrared absorption. The air-filled window performs as well as an uncoated, NH_3-filled window. Natural convection is not

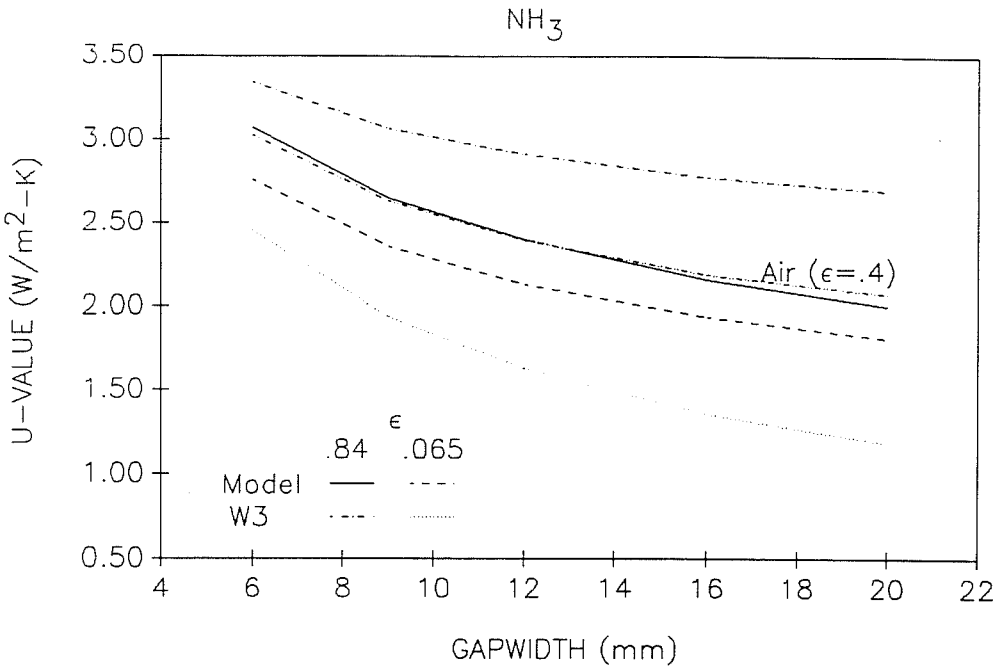

Fig. 7. *U*-values calculated by the finite-element model and WINDOW 3.1 for horizontal windows filled with NH_3. Also included, are WINDOW 3.1 *U*-values for horizontal windows filled with air which have a low-emittance coating ($\epsilon = 0.4$).

included, but one can speculate that the effect of natural convection on the performance of both windows would be approximately the same.

4. Conclusions

We developed a model to study the coupled effects of radiation and conduction through infrared absorbing gasses separating window glazing layers. For small vertical gap widths and for windows heated from above, where convection is negligible, our model agrees well with experimental data. For larger vertical gap widths, where energy savings from the use of infrared absorbing gasses may begin to accrue, convection effects will begin to take effect and negate the positive impact of going to larger gap widths.

Low-emittance coatings are much more effective at reducing infrared radiation heat transfer than IR absorbing gasses. Gasses for gas-filling should be chosen for their low conductivity and high kinematic viscosity in order to effectively reduce conductive/convective heat transfer. The effective use of infrared absorbing gasses is thus limited to horizontal windows heated from above, or to thin gaps where low-emittance coatings cannot be used.

Modeling the performance of common infrared absorbing gasses used in window applications (i.e. CO_2 and SF_6) can be undertaken to an accuracy of within 10% (and usually less) without considering IR absorption within the gas space. This

allows for much simpler models and a more accurate treatment of convective (usually more important) effects.

Acknowledgement

This work was supported by the Assistant Secretary for Conservation and Renewable Energy, Office of Buildings and Community Systems, Building Systems Division of the US Department of Energy under Contract No. DE-AC01-76SF00098.

References

[1] M. Rubin, Energy Res. 6 (1982) 341.
[2] J.L. Wright and H.F. Sullivan, VISION: A Computer Program to Evaluate the Thermal Performance of Innovative Glazing Systems Reference Manual, Dept. of Mech. Engineering, University of Waterloo, Ontario, Canada.
[3] H.J. Glaser, Glastechnische Ber. 50 (1977) 248.
[4] T.S. Eriksson and C.G. Granqvist, Sol. Energy Mater. 16 (1987) 243.
[5] R. Siegal and J.R. Howell, Thermal Radiation Heat Transfer (Hemisphere, New York, 1981).
[6] D.K. Edwards and A. Balakrishnan, Int. J. Heat Mass Transfer 16 (1973) 25.
[7] S. Reilly, M. Rubin, A. Tuntomo and C.L. Tien, Infrared Radiation of SF_6 and Its Application to Gas-Filled Double-Pane Windows, Experimental Heat Transfer, submitted.
[8] C.L. Tien, Int. J. Heat Mass Transfer 16 (1973) 856.
[9] C.L. Tien, M.F. Modest and C.R. McCreight, J. Quant. Spectrosc. Radiat. Transfer 12 (1972) 267.
[10] J.D. Felske and C.L. Tien, J. Quant. Spectrosc. Radiat. Transfer 14 (1974) 35.
[11] D.K. Arasteh, M.S. Reilly and M.D. Rubin, ASHRAE Trans. 95 (1989).
[12] D.K. Edwards, J. Heat Transfer (February 1962) 1.
[13] D.S. Dunn, K. Scanlon and J. Overend, Spectrochim. Acta 38A (1982) 841.
[14] J.A. Wiebelt, Engineering Heat Transfer (Holt, Rinehart and Winston, New York, 1966).
[15] D. Arasteh, J. Hartmann and M. Rubin, ASHRAE Trans. Part 1, 93 (1987) 1425.
[16] D.M. Kim and R. Viskanta, Numerical Heat Transfer 7 (1984) 449.
[17] D. Arasteh, S. Selkowitz and J.R. Wolfe, J. Sol. Energy Eng. 111 (1989) 44.